
Prospective Comparison of PET Imaging with PSMA-Targeted ^{18}F -DCFPyL Versus Na^{18}F for Bone Lesion Detection in Patients with Metastatic Prostate Cancer

Steven P. Rowe^{1,2}, Xin Li^{1,3}, Bruce J. Trock², Rudolf A. Werner^{1,4}, Sarah Frey¹, Michael DiGianvittorio^{1,5}, J. Keith Bleiler⁶, Diane K. Reyes², Rehab Abdallah¹, Kenneth J. Pienta², Michael A. Gorin^{1,2}, and Martin G. Pomper^{1,2}

¹Russell H. Morgan Department of Radiology and Radiological Science, Johns Hopkins University School of Medicine, Baltimore, Maryland; ²James Buchanan Brady Urological Institute and Department of Urology, Johns Hopkins University School of Medicine, Baltimore, Maryland; ³Department of Radiology, Shandong Provincial Hospital, Shandong University, Jinan City, Shandong Province, China; ⁴Department of Nuclear Medicine, University Hospital Wurzburg, Wurzburg, Germany; ⁵Spectrum Medical Group, South Portland, Maine; and ⁶Greater Boston Urology, Dedham, Massachusetts

Bone metastases in prostate cancer (PCa) have important prognostic significance, and imaging modalities used for PCa staging should have high sensitivity for detecting such lesions. Prostate-specific membrane antigen (PSMA)-targeted PET radiotracers are promising new agents for imaging PCa. We undertook a head-to-head comparison of PSMA-targeted 2-(3-{1-carboxy-5-[(6- ^{18}F -fluoro-pyridine-3-carbonyl)-amino]-pentyl)-ureido)-pentanedioic acid (^{18}F -DCFPyL) PET to Na^{18}F PET to determine which modality was more sensitive for the detection of lesions suggestive of bone metastases in a group of patients with metastatic PCa. **Methods:** Patients with progressive, metastatic PCa were prospectively imaged with both ^{18}F -DCFPyL and Na^{18}F PET/CT, with both scans occurring within 24 h of each other. A consensus 2-reader central review was performed to identify all bone lesions suggestive of sites of PCa involvement on both scans, and maximized SUVs corrected for body weight (SUV_{max}) and lean body mass (SUL_{max}) were recorded. Soft-tissue lesions were also noted on both scans, and SUV_{max} , SUL_{max} , and PSMA reporting and data system (RADS) version 1.0 scores were recorded. Data from the 2 scans were compared using a generalized estimating equation. **Results:** In total, 16 patients meeting all inclusion criteria were enrolled in this study, and 15 of the 16 (93.8%) were imaged with both PET radiotracers. In total, 405 bone lesions suggestive of sites of PCa were identified on at least 1 scan. On ^{18}F -DCFPyL PET/CT, 391 (96.5%) were definitively positive, 4 (1.0%) were equivocally positive, and 10 (2.5%) were negative. On Na^{18}F PET/CT, the corresponding values were 388 (95.8%), 4 (1.0%), and 13 (3.2%). Of the definitively negative lesions on ^{18}F -DCFPyL PET, 8 of 10 (80.0%) were sclerotic and 2 of 10 (20.0%) were infiltrative or marrow-based. Additionally, 12 of 13 (92.3%) of the definitively negative lesions on Na^{18}F PET were infiltrative or marrow-based and 1 of 13 (7.7%) was lytic. Also identified were 78 PSMA-RADS-4, 17 PSMA-RADS-5, and 1 PSMA-RADS-3C soft-tissue lesions. **Conclusion:** PET/CT imaging using ^{18}F -DCFPyL and Na^{18}F PET had nearly identical sensitivities for the detection of bone lesions in patients with metastatic PCa. As would be expected, PSMA-targeted PET provides more information on

soft-tissue disease. There may be little additional value to imaging PCa patients with Na^{18}F after a PSMA-targeted PET scan has already been performed.

Key Words: prostate-specific membrane antigen; PSMA; prostate cancer; bone metastases; ^{18}F Na; PyL; PET/CT

J Nucl Med 2020; 61:183–188

DOI: 10.2967/jnumed.119.227793

Prostate cancer (PCa) is the most common noncutaneous malignancy in men (1) and frequently metastasizes to bone (2). Despite the considerable importance of accurately identifying patients with bone metastases, anatomic imaging with CT or functional imaging with $^{99\text{m}}\text{Tc}$ -methylene diphosphonate bone scans have generally shown poor sensitivity for identifying such metastases (3). The relatively low sensitivity of conventional imaging modalities for detecting bone metastases from PCa has prompted an extensive search for tumor-specific PET imaging agents (4). Prostate-specific membrane antigen (PSMA) is a type II transmembrane glycoprotein that is highly expressed by PCa epithelial cells (5–7). Small-molecule ligands that bind to the active site of PSMA and are labeled with radionuclides for PET imaging including ^{18}F (8–10) and ^{68}Ga (11,12) have been extensively investigated as molecular imaging agents for PCa. Our group has focused primarily on ^{18}F -labeled radiotracers because of their favorable imaging characteristics, including a near-ideal 110-min half-life and low positron energy leading to short path-length annihilation and intrinsic high spatial resolution (13,14).

Previously we have shown that the PSMA-targeted PET radiotracer 2-(3-{1-carboxy-5-[(6- ^{18}F -fluoro-pyridine-3-carbonyl)-amino]-pentyl)-ureido)-pentanedioic acid (^{18}F -DCFPyL) (9) offers a superior lesion detection rate in patients with metastatic PCa as compared with conventional imaging with CT and bone scans (15). Additionally, we have observed a markedly higher bone lesion detection rate with ^{18}F -DCFPyL than with Na^{18}F in a single patient with aggressive castration-resistant metastatic PCa (16). In light of these observations, we sought to further explore the relative detection efficiencies of ^{18}F -DCFPyL PET/CT and Na^{18}F PET/CT for detecting bony metastases in a prospective head-to-head comparative study.

Received Mar. 13, 2019; revision accepted Jul. 12, 2019.

For correspondence or reprints contact: Steven P. Rowe, Johns Hopkins University, School of Medicine, 601 N. Caroline St., JHOC 3233, Baltimore, MD 21287.

E-mail: srowe8@jhmi.edu

Published online Aug. 26, 2019.

COPYRIGHT © 2020 by the Society of Nuclear Medicine and Molecular Imaging.

MATERIALS AND METHODS

Patient Population

This prospective study (Fig. 1) was approved by the Institutional Review Board of Johns Hopkins Medicine. All participants gave written informed consent and were imaged under a U.S. Food and Drug Administration Investigational New Drug application (121064; ClinicalTrials.gov identifier NCT03497377). Key inclusion criteria were a history of histologic confirmation of PCa; radiologic evidence of new or progressive metastatic PCa on CT, MRI, bone scans, Na¹⁸F PET, or ¹⁸F-FDG PET; and a rising level of prostate-specific antigen on at least 2 observations taken at least 1 wk apart. Patients could remain on androgen deprivation therapy provided they were on the same regimen before documentation of progressive metastatic disease. Key exclusion criteria were a history of being treated with an investigational drug, biologic, or therapeutic device within 14 d before initial study radiotracer administration; prior radiation or chemotherapy within 2 wk before initial study radiotracer administration; initiation of new therapy for progressive metastatic disease since radiographic documentation of progression; serum creatinine or total bilirubin higher than 3 times the upper limit of normal; or liver transaminases higher than 5 times the upper limit of normal.

Imaging Protocol

All patients were imaged with ¹⁸F-DCFPyL and Na¹⁸F within 24 h. Patients were imaged on either a Biograph mCT 128-slice PET/CT scanner (Siemens Healthineers) or a Discovery RX 64-slice PET/CT scanner (GE Healthcare). For each individual patient, both scans were performed on the same scanner. For the ¹⁸F-DCFPyL scans, patients were intravenously injected with no more than 333 MBq (9 mCi) of radiotracer approximately 60 min before image acquisition. For the Na¹⁸F scans, patients were intravenously injected with approximately 370 MBq (10 mCi) of radiotracer approximately 60 min before image acquisition. Regardless of the administered radiotracer, the scanners were operated in 3-dimensional emission mode with CT attenuation correction, and images were reconstructed with manufacturer-supplied ordered-subset expectation maximization iterative methods without point-spread function. The field of view was vertex to mid thigh for ¹⁸F-DCFPyL and vertex to toes for Na¹⁸F.

Image Analysis

All PET/CT scans were collaboratively reviewed by 2 board-certified nuclear medicine specialists with experience in both ¹⁸F-DCFPyL

and Na¹⁸F PET/CT interpretation. A consensus was reached by the reviewers as to the presence of definitive or equivocal lesions on the basis of focal abnormal radiotracer uptake above the background level and outside the expected biodistribution of each radiotracer. The readers evaluated the images from both radiotracers together so as to determine the lesion-level concordance and discordance of the 2 agents. Degenerative change and suspected false-positive lesions were not included in the analysis (Fig. 2; Supplemental Fig. 1 [supplemental materials are available at <http://jnm.snmjournals.org>]). For each lesion, the maximum SUV was determined for body weight (SUV_{max}) and lean body mass (SUL_{max}). A spheric volume of interest was also placed over a non-disease-involved site in the right femur such that the maximum area of the sphere on an axial slice matched the axial cross-sectional area of the femur on the same slice. These femur volumes of interest were acquired so that uptake in lesions could be normalized to take into account the intrinsically higher uptake of Na¹⁸F in bone. Soft-tissue lesions were also noted on both scans, with SUV_{max} and SUL_{max} recorded for those lesions appreciated on ¹⁸F-DCFPyL PET. All detected lesions were also assigned a PSMA reporting and data system (PSMA-RADS) score (17–20).

Statistical Analysis

Because of the mostly descriptive nature of this study, a formal power calculation was not performed. Rather, a sample size of 16 patients was chosen on the basis of the availability of study funding. Descriptive statistics were used for patient demographics and clinical information, the number of lesions identified on each PET modality, and the median and interquartile ranges (IQRs) of the uptake parameters for the bone lesions.

SUV_{max} and SUL_{max} were normalized by dividing each observation by the mean right femur measurement for that patient, followed by natural log transformation of each normalized value. ¹⁸F-DCFPyL and Na¹⁸F PET studies were compared for both SUV_{max} and SUL_{max} (separately) using these log-transformed values in a generalized estimating equation linear regression model, where ¹⁸F-DCFPyL SUV_{max} or SUL_{max} was the independent variable and Na¹⁸F SUV_{max} or SUL_{max} was the dependent variable. When considering lesion detection by either method, dichotomized as definitively positive versus equivocal or definitively negative, a generalized estimating equation logistic regression model was used (21). Two patients had a disproportionately large number of lesions detected (160 and 155 total lesions). In contrast, among the other 14 patients the mean number of lesions was 6.9. Therefore, we repeated the generalized estimating equation linear and logistic regression analyses after excluding those 2 patients.

RESULTS

Between May and November 2016, 16 patients who met all predetermined inclusion criteria were enrolled and imaged in this study, with 1 patient refusing to undergo Na¹⁸F PET/CT after having already been imaged with ¹⁸F-DCFPyL PET/CT (Fig. 1). An additional 9 screened patients did not meet all inclusion criteria. Supplemental Table 1 lists key demographic and clinical information from the patients in this study. Patients had a mean age of 65.8 y (range, 52–77 y), and 14 of 16 (87.5%) patients were white. At the time of imaging, 14 of 16 (87.5%) patients had been treated,

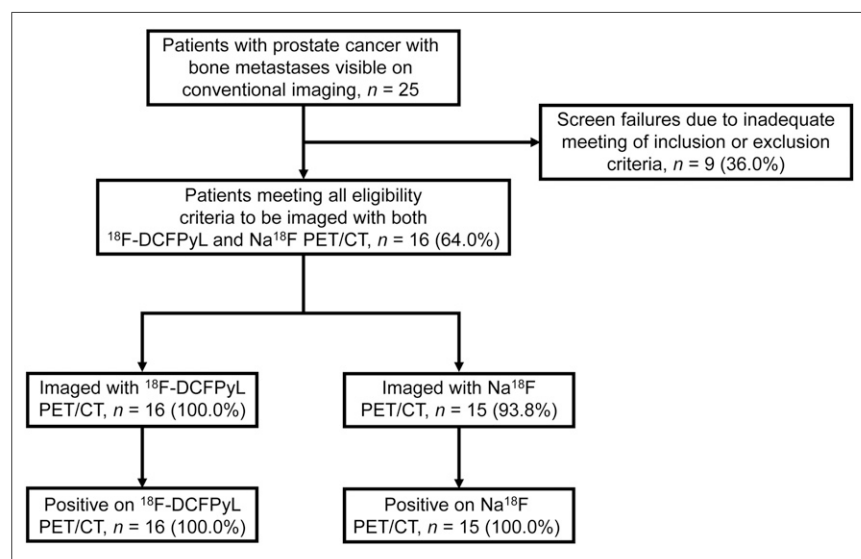


FIGURE 1. Standards for Reporting of Diagnostic Accuracy Studies (STARD) flow diagram.

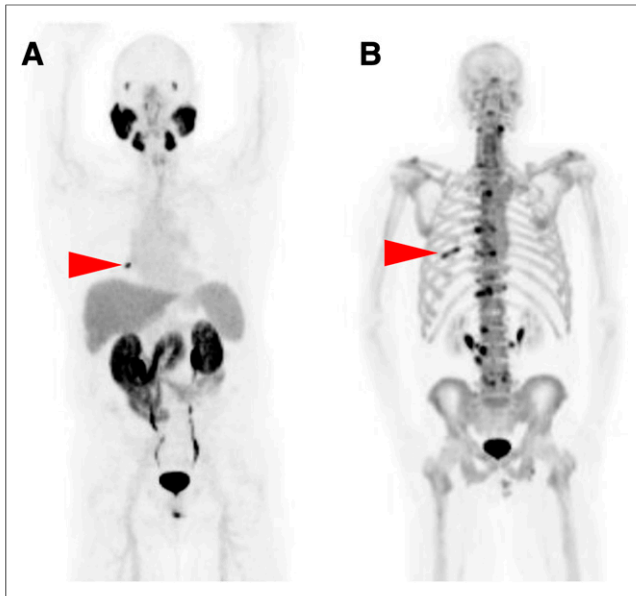


FIGURE 2. Anterior maximum-intensity projections for both ^{18}F -DCFPyL (A) and Na^{18}F PET/CT (B) demonstrate single bone lesion (arrowheads) suggestive of metastatic disease in right eighth rib. Extensive abnormal uptake in spine on Na^{18}F PET image was attributed to degenerative change by central reviewers.

or were being treated, with systemic therapy. The details of the prior or current therapies for the patients are included in Table 1. All patients were in grade group 2 or higher at original diagnosis (6/16 [37.5%] grade group 2–3, 4/16 [25.0%] grade group 4, and 6/16 [37.5%] grade group 5). The median serum prostate-specific antigen level at the time of imaging was 4.4 ng/mL (range, 0.2–224.5 ng/mL), and 10 of 16 (62.5%) patients had undetectable levels of testosterone on current therapy.

After review by the 2 readers, 405 bone lesions suggestive of sites of PCa involvement were identified on at least one of the modalities. The patient who refused Na^{18}F imaging was excluded from the imaging portion of the analysis. The numbers of positive, equivocal, and negative lesions with each modality for each patient are tabulated in Supplemental Table 1. With regard to CT morphology, 275 (67.9%) of the lesions were sclerotic, 121 (29.9%) were infiltrative or marrow-based, and 9 (2.2%) were lytic. On ^{18}F -DCFPyL PET, 391 (96.5%) were definitively positive, 4 (1.0%) were equivocally positive, and 10 (2.5%) were negative. On Na^{18}F PET, 388 (95.8%) were definitively positive, 4 (1.0%)

were equivocally positive, and 13 (3.2%) were negative. Of the definitively negative lesions on ^{18}F -DCFPyL PET, 8 of 10 (80.0%) were sclerotic and 2 of 10 (20.0%) were infiltrative or marrow-based. Conversely, 12 of 13 (92.3%) of the definitively negative lesions on Na^{18}F PET were infiltrative or marrow-based, whereas 1 of 13 (7.7%) was lytic. Additional details on bone lesion detection by the modalities are found in Tables 1 and 2 and in Supplemental Table 2. Relevant examples of discordant findings between the 2 PET scans are shown in Figures 3 and 4. Additional representative images from patients with varying disease burdens are shown in Supplemental Figure 2.

For those lesions that were definitively or equivocally positive on ^{18}F -DCFPyL, the median SUV_{max} was 7.4 (IQR, 4.2–12.9) and the median SUL_{max} was 5.5 (IQR, 3.2–9.5). For those lesions that were definitively or equivocally positive on Na^{18}F PET, the median SUV_{max} was 18.0 (IQR, 11.5–29.3) and the median SUL_{max} was 13.4 (IQR, 8.7–22.6).

In total, 11 of 15 (73.3%) patients had soft-tissue findings suggestive of sites of PCa on ^{18}F -DCFPyL PET/CT. The CT portion of the Na^{18}F PET/CT demonstrated at least 1 suggestive soft-tissue finding in 6 of 15 (40.0%) patients. All suggestive soft-tissue findings on Na^{18}F PET/CT were found to have uptake on ^{18}F -DCFPyL PET/CT, and all patients with such findings had evidence of more widespread soft-tissue involvement on ^{18}F -DCFPyL PET/CT. In total, 78 PSMA-RADS-4 lesions were identified on ^{18}F -DCFPyL PET/CT (i.e., sites of uptake suggestive of PCa involvement without a corresponding CT abnormality), with a range of 0–18 lesions per patient. Correspondingly, 17 PSMA-RADS-5 lesions were identified on ^{18}F -DCFPyL PET/CT with CT abnormalities on Na^{18}F PET/CT, with a range from 0–7 lesions per patient. One additional soft-tissue finding (a thyroid nodule) was categorized as PSMA-RADS-3C (i.e., a finding with uptake that is suggestive of a non-PCa malignancy). In the analysis of SUVs, we observed a statistically significant positive linear association between the natural logarithm of normalized (LnN) ^{18}F -DCFPyL SUV_{max} and LnN Na^{18}F SUV_{max} (slope, 0.638; 95% confidence interval [CI], 0.493–0.783; $P < 0.0001$) among definitively and equivocally positive lesions. There was also a statistically significant positive linear association between LnN ^{18}F -DCFPyL SUL_{max} and LnN Na^{18}F SUL_{max} (slope, 0.636; 95% CI, 0.494–0.779; $P < 0.0001$). When the 2 patients with the largest number of lesions (160 and 155 lesions) were excluded, the statistically significant positive correlations between the uptake parameters remained: the positive linear association between LnN ^{18}F -DCFPyL SUV_{max} and LnN Na^{18}F SUV_{max} demonstrated a slope of 0.877 (95% CI,

TABLE 1
Number of Each Type of CT Morphologic Lesion Detected by ^{18}F -DCFPyL and Na^{18}F PET

| Modality | Lesion morphology on CT | Definitively positive for uptake on PET | Equivocally positive for uptake on PET | Negative for uptake on PET |
|------------------------------|---------------------------|---|--|----------------------------|
| ^{18}F -DCFPyL PET | Sclerotic | 263 | 4 | 8 |
| | Infiltrative/marrow-based | 119 | 0 | 2 |
| | Lytic | 9 | 0 | 0 |
| Na^{18}F PET | Sclerotic | 272 | 2 | 0 |
| | Infiltrative/marrow-based | 108 | 2 | 12 |
| | Lytic | 8 | 0 | 1 |

TABLE 2

Two-by-Two Table Comparing Lesion Detection Between ¹⁸F-DCFPyL and Na¹⁸F PET

| ¹⁸ F-DCFPyL | Na ¹⁸ F | |
|------------------------|--------------------|----------|
| | Positive | Negative |
| Positive | 382 | 13 |
| Negative | 10 | NA |

NA = not applicable.

Equivocal lesions were considered positive for this comparison.

0.753–0.9998; $P < 0.0001$), and the positive linear association between LnN ¹⁸F-DCFPyL SUL_{max} and LnN Na¹⁸F SUL_{max} demonstrated a slope of 0.765 (95% CI, 0.669–0.861; $P < 0.0001$).

With regard to lesion detection, 380 of 405 (93.8%) observations were exactly concordant between ¹⁸F-DCFPyL and Na¹⁸F. When detection was dichotomized as definitively positive versus equivocal or definitively negative, the odds ratio from the generalized estimating equation model was statistically significant (odds ratio, 4.32; 95% CI, 1.04–18.06; $P = 0.045$). This indicates that a definitively positive lesion on the ¹⁸F-DCFPyL PET scan predicts an approximately 4-fold higher likelihood that the lesion would be definitively positive on Na¹⁸F. After excluding the 2 patients with a disproportionately large number of lesions, the results were very similar (odds ratio, 4.01; 95% CI, 0.96–16.74; $P = 0.057$).

DISCUSSION

In this prospective study of 16 patients with metastatic PCa, the PSMA-targeted radiotracer ¹⁸F-DCFPyL showed sensitivity similar to that of Na¹⁸F for detection of suspected bone lesions, and uptake within those lesions correlated strongly between the 2 modalities. Although this overall result differs from our previously reported case report comparing these 2 modalities in a single patient (16), it is in keeping with some recent reports that have investigated similar hypotheses. For example, Zacho et al. recently performed a prospective study on 68 patients with

biochemically recurrent PCa and found that Na¹⁸F and a ⁶⁸Ga-labeled PSMA-targeted PET radiotracer had similarly high rates for identifying PCa bone metastases (22). Further, a patient-level analysis by Dyrberg et al. of patients with PCa undergoing imaging with both Na¹⁸F and a ⁶⁸Ga-labeled PSMA-targeted PET radiotracer also found no difference in diagnostic ability between the agents (23).

Other studies have found Na¹⁸F to be advantageous for the detection of bone lesions relative to PSMA-targeted radiotracers. Harmon et al. used the PSMA-targeted agent ¹⁸F-DCFBC in a prospective comparison to Na¹⁸F and found significantly fewer bone lesions in patients with relatively less advanced disease, although findings between the 2 radiotracers were similar in advanced metastatic castration-resistant PCa (24). In that study, the use of ¹⁸F-DCFBC, an agent with high blood-pool activity and lower tumor-to-background ratios than most other PSMA-targeted agents being investigated, may have led to limited lesion detectability relative to Na¹⁸F (3). Interestingly, another study that compared a ⁶⁸Ga-labeled PSMA-targeted PET radiotracer to Na¹⁸F also found a lower rate of lesion detection with the PSMA-targeted compound (25). For the patients in that study, radionuclide therapy with either ¹⁷⁷Lu-PSMA-617 or ²²³Ra was being planned, and many of the patients had been pretreated with systemic therapy before the PET scans (25). This may have led to a proportion of the lesions in those patients being effectively treated or healed, limiting the detection efficiency of a tumor-specific radiotracer such as a PSMA-targeted agent.

Expanding on that idea, a potential reason for the relatively similar rates of lesion detection in our current study, compared with our previous case report suggesting that a PSMA-targeted agent would detect more lesions (16), may lie in the type of patients being imaged, how aggressive the phenotypes of their disease were, and the degree to which they had been pretreated. Patients with very aggressive disease that is rapidly progressing may have a disproportionate number of infiltrative or marrow-based bone metastases that are better detected on PSMA-targeted PET. Those patients whose disease course is very advanced may have some bone metastases that have been effectively treated, leading to loss of uptake of PSMA-targeted radiotracers despite persistent uptake of Na¹⁸F, thus producing a higher lesion detection efficiency for Na¹⁸F. It is also possible that a proportion of such heavily treated patients may have had neuroendocrine differentiation, which is known to lead to downregulation of PSMA and decreased uptake of radiotracers targeting this tumor marker (26).

Beyond bone lesion detection, PSMA-targeted radiotracers offer the distinct advantage relative to Na¹⁸F of characterizing soft-tissue lesions. This was certainly the case in this cohort. Most of the patients had evidence of soft-tissue PCa involvement, and in every one of those patients the soft-tissue sites were either exclusively appreciable on ¹⁸F-DCFPyL PET or more sites of disease were seen with the PSMA-targeted agent. In addition to the PSMA-RADS-4 lesions that were seen only on the ¹⁸F-DCFPyL PET scan (such as subcentimeter

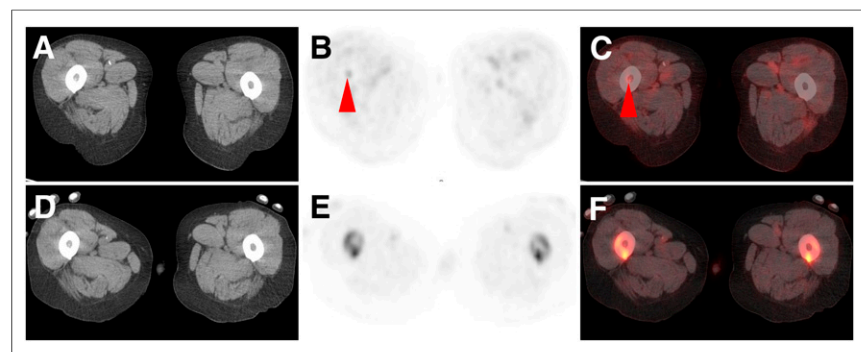


FIGURE 3. CT (A), ¹⁸F-DCFPyL PET (B), ¹⁸F-DCFPyL PET/CT (C) and, at same level, CT (D), Na¹⁸F PET (E), and Na¹⁸F PET/CT (F) axial images of patient with widely metastatic PCa. Both modalities showed numerous lesions, but only ¹⁸F-DCFPyL shows uptake (subtle but definitively present and suggestive) in proximal right femur marrow space (arrowheads). This type of lesion constituted most lesions not appreciable with Na¹⁸F PET in this study.

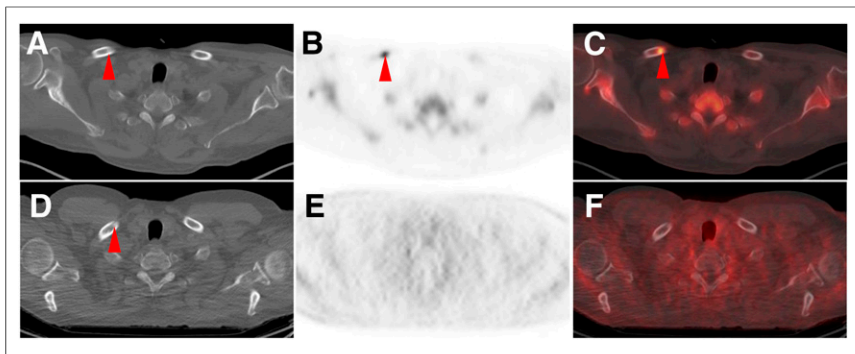


FIGURE 4. CT (A), Na¹⁸F PET (B), Na¹⁸F PET/CT (C) and, at same level, CT (D), ¹⁸F-DCFPyL PET (E), and ¹⁸F-DCFPyL PET/CT (F) axial images of patient with widely metastatic PCa. Both modalities show subtle sclerotic lesion in right clavicle (arrowheads), but only Na¹⁸F shows associated intense uptake compatible with site of PCa. Most lesions with Na¹⁸F uptake that lacked ¹⁸F-DCFPyL uptake were sclerotic.

lymph nodes; and, by definition, PSMA-RADS-4 lymph nodes should not be appreciable with a non-tumor-specific radiotracer given that they are not abnormal on anatomic imaging), a single PSMA-RADS-3C lesion (17,18) that was suspected (although indeterminate) of being a coexisting malignancy was also noted in 1 patient, demonstrating the ability of PSMA-targeted agents to have uptake in non-PCa malignancies (27).

As with any study, there are limitations to the presented work. Although this was a prospective study, it was a single-center experience with a relatively small number of enrolled patients. Further, all but 2 of the patients had received at least 1 line of systemic therapy, making this a relatively heavily pre-treated patient population, potentially confounding the analysis of active versus treated lesions on Na¹⁸F. We believe the large number of lesions in the lesion-by-lesion analysis ameliorates some of the disadvantage of having relatively few patients. For these reasons, head-to-head studies of PSMA-targeted radiotracers versus Na¹⁸F with patients carefully stratified by prior therapy may help clarify the respective roles of these radiotracers in patients with a variety of disease states. Furthermore, given the relatively widespread disease in these patients, there was no specific standard of care for obtaining tissue confirmation of lesions, and that lack of available histology is another limitation of this study.

CONCLUSION

PSMA-targeted ¹⁸F-DCFPyL PET has nearly identical sensitivity to Na¹⁸F PET for detecting bone lesions suggestive of PCa in patients with known metastatic disease. However, a unique benefit of PSMA-targeted PET is the ability to image soft-tissue sites of metastasis. Together, these findings argue in favor of the routine use of PSMA-targeted PET imaging in place of Na¹⁸F PET for this patient population. Expanding these conclusions to other disease states (e.g., biochemical recurrence) will require further study.

DISCLOSURE

We acknowledge funding from CA134675, CA183031, CA184228, EB024495, the Prostate Cancer Foundation Young Investigator Award, and the European Union's Horizon 2020 research and innovation program under Marie Skłodowska-Curie grant

agreement 701983. Martin Pomper is a coinventor on a U.S. patent covering ¹⁸F-DCFPyL and as such is entitled to a portion of any licensing fees and royalties generated by this technology. This arrangement has been reviewed and approved by the Johns Hopkins University in accordance with its conflict-of-interest policies. Steven Rowe is a consultant to Progenics Pharmaceuticals, the licensee of ¹⁸F-DCFPyL. Michael Gorin has served as a consultant to Progenics Pharmaceuticals. Steven Rowe, Michael Gorin, Kenneth Pienta, and Martin Pomper receive research funding from Progenics Pharmaceuticals. No other potential conflict of interest relevant to this article was reported.

KEY POINTS

QUESTION: How does the sensitivity of the PSMA-targeted PET radiotracer ¹⁸F-DCFPyL compare with Na¹⁸F PET for bone lesion detection in patients with metastatic PCa?

PERTINENT FINDINGS: In a prospective head-to-head comparison of ¹⁸F-DCFPyL PET versus Na¹⁸F PET in 16 patients with metastatic PCa, the 2 agents detected a nearly identical number of bone lesions (395 positive and equivocal lesions on ¹⁸F-DCFPyL PET and 392 positive and equivocal lesions on Na¹⁸F PET). There was no statistically significant difference in bone lesion detection efficiency between the 2 modalities. ¹⁸F-DCFPyL PET does, however, provide additional information regarding soft-tissue findings.

IMPLICATIONS FOR PATIENT CARE: These findings argue in favor of the routine use of PSMA-targeted PET imaging in place of Na¹⁸F PET for bone lesion detection in the staging of PCa patients, once PSMA-targeted agents such as ¹⁸F-DCFPyL achieve regulatory approval.

REFERENCES

1. Siegel RL, Miller KD, Jemal A. Cancer statistics, 2018. *CA Cancer J Clin*. 2018; 68:7–30.
2. Gandaglia G, Karakiewicz PI, Briganti A, et al. Impact of the site of metastases on survival in patients with metastatic prostate cancer. *Eur Urol*. 2015;68:325–334.
3. Rowe SP, Macura KJ, Ciarallo A, et al. Comparison of prostate-specific membrane antigen-based ¹⁸F-DCFBC PET/CT to conventional imaging modalities for detection of hormone-naïve and castration-resistant metastatic prostate cancer. *J Nucl Med*. 2016;57:46–53.
4. Li R, Ravizzini GC, Gorin MA, et al. The use of PET/CT in prostate cancer. *Prostate Cancer Prostatic Dis*. 2018;21:4–21.
5. Ross JS, Sheehan CE, Fisher HA, et al. Correlation of primary tumor prostate-specific membrane antigen expression with disease recurrence in prostate cancer. *Clin Cancer Res*. 2003;9:6357–6362.
6. Marchal C, Redondo M, Padilla M, et al. Expression of prostate specific membrane antigen (PSMA) in prostatic adenocarcinoma and prostatic intraepithelial neoplasia. *Histol Histopathol*. 2004;19:715–718.
7. Perner S, Hofer MD, Kim R, et al. Prostate-specific membrane antigen expression as a predictor of prostate cancer progression. *Hum Pathol*. 2007;38:696–701.
8. Cho SY, Gage KL, Mease RC, et al. Biodistribution, tumor detection, and radiation dosimetry of ¹⁸F-DCFBC, a low-molecular-weight inhibitor of prostate-specific membrane antigen, in patients with metastatic prostate cancer. *J Nucl Med*. 2012;53:1883–1891.

9. Szabo Z, Mena E, Rowe SP, et al. Initial evaluation of [¹⁸F]DCFPyL for prostate-specific membrane antigen (PSMA)-targeted PET imaging of prostate cancer. *Mol Imaging Biol.* 2015;17:565–574.
10. Giesel FL, Hadaschik B, Cardinale J, et al. F-18 labelled PSMA-1007: biodistribution, radiation dosimetry and histopathological validation of tumor lesions in prostate cancer patients. *Eur J Nucl Med Mol Imaging.* 2017;44:678–688.
11. Afshar-Oromieh A, Malcher A, Eder M, et al. PET imaging with a [⁶⁸Ga]galium-labelled PSMA ligand for the diagnosis of prostate cancer: biodistribution in humans and first evaluation of tumour lesions. *Eur J Nucl Med Mol Imaging.* 2013;40:486–495.
12. Afshar-Oromieh A, Hetzheim H, Kratochwil C, et al. The theranostic PSMA ligand PSMA-617 in the diagnosis of prostate cancer by PET/CT: biodistribution in humans, radiation dosimetry, and first evaluation of tumor lesions. *J Nucl Med.* 2015;56:1697–1705.
13. Sanchez-Crespo A. Comparison of gallium-68 and fluorine-18 imaging characteristics in positron emission tomography. *Appl Radiat Isot.* 2013;76:55–62.
14. Gorin MA, Pomper MG, Rowe SP. PSMA-targeted imaging of prostate cancer: the best is yet to come. *BJU Int.* 2016;117:715–716.
15. Rowe SP, Macura KJ, Mena E, et al. PSMA-based [¹⁸F]DCFPyL PET/CT is superior to conventional imaging for lesion detection in patients with metastatic prostate cancer. *Mol Imaging Biol.* 2016;18:411–419.
16. Rowe SP, Mana-Ay M, Javadi MS, et al. PSMA-based detection of prostate cancer bone lesions with ¹⁸F-DCFPyL PET/CT: a sensitive alternative to (^{99m}Tc-MDP bone scan and Na¹⁸F PET/CT? *Clin Genitourin Cancer.* 2016;14:e115–e118.
17. Rowe SP, Pienta KJ, Pomper MG, Gorin MA. Proposal for a structured reporting system for prostate-specific membrane antigen-targeted PET imaging: PSMA-RADS version 1.0. *J Nucl Med.* 2018;59:479–485.
18. Rowe SP, Pienta KJ, Pomper MG, Gorin MA. PSMA-RADS version 1.0: a step towards standardizing the interpretation and reporting of PSMA-targeted PET imaging studies. *Eur Urol.* 2018;73:485–487.
19. Yin Y, Werner RA, Higuchi T, et al. Follow-up of lesions with equivocal radio-tracer uptake on PSMA-targeted PET in patients with prostate cancer: predictive values of the PSMA-RADS-3A and PSMA-RADS-3B categories. *J Nucl Med.* 2019;60:511–516.
20. Werner RA, Bundschuh RA, Bundschuh L, et al. Interobserver agreement for the standardized reporting system PSMA-RADS 1.0 on ¹⁸F-DCFPyL PET/CT imaging. *J Nucl Med.* 2018;59:1857–1864.
21. Hanley JA, Negassa A, Edwards MD, Forrester JE. Statistical analysis of correlated data using generalized estimating equations: an orientation. *Am J Epidemiol.* 2003;157:364–375.
22. Zacho HD, Nielsen JB, Afshar-Oromieh A, et al. Prospective comparison of ⁶⁸Ga-PSMA PET/CT, ¹⁸F-sodium fluoride PET/CT and diffusion weighted-MRI at for the detection of bone metastases in biochemically recurrent prostate cancer. *Eur J Nucl Med Mol Imaging.* 2018;45:1884–1897.
23. Dyrberg E, Hendel HW, Huynh THV, et al. ⁶⁸Ga-PSMA-PET/CT in comparison with ¹⁸F-fluoride-PET/CT and whole-body MRI for the detection of bone metastases in patients with prostate cancer: a prospective diagnostic accuracy study. *Eur Radiol.* 2019;29:1221–1230.
24. Harmon SA, Bergvall E, Mena E, et al. A prospective comparison of ¹⁸F-sodium fluoride PET/CT and PSMA-targeted ¹⁸F-DCFBC PET/CT in metastatic prostate cancer. *J Nucl Med.* 2018;59:1665–1671.
25. Uprimny C, Sviridenka A, Fritz J, et al. Comparison of [⁶⁸Ga]Ga-PSMA-11 PET/CT with [¹⁸F]NaF PET/CT in the evaluation of bone metastases in metastatic prostate cancer patients prior to radionuclide therapy. *Eur J Nucl Med Mol Imaging.* 2018;45:1873–1883.
26. Tosoian JJ, Gorin MA, Rowe SP, et al. Correlation of PSMA-targeted ¹⁸F-DCFPyL PET/CT findings with immunohistochemical and genomic data in a patient with metastatic neuroendocrine prostate cancer. *Clin Genitourin Cancer.* 2017;15:e65–e68.
27. Salas Fragomeni RA, Amir T, Sheikhabaei S, et al. Imaging of nonprostate cancers using PSMA-targeted radiotracers: rationale, current state of the field, and a call to arms. *J Nucl Med.* 2018;59:871–877.